JOURNAL OF APPLIED PHYSICS VOLUME 39, NUMBER 10 SEPTEMBER 1968

Material Strength Effect in the Shock Compression of Alumina*

THOMAS J. AHRENS†
Stanford Research Institute, Menlo Park, California and *Division of Geological Sciences, California Institute of Technology, Pasadena, California*

AND

W. H. GUST AND E. B. ROYCE
Lawrence Radiation Laboratory, University of California, Livermore, California

(Received 16 February 1968; in final form 24 May 1968)

The Hugoniot elastic limits (HEL) of a high-density aluminum oxide ceramic (Lucalox) and a slightly lower-density ceramic (porosity approximately 4%) were determined to be 112±13 and 83±5 kbar, respectively. Above the HEL, the shock-stress–volume Hugoniot curves for both materials are offset by 40 kbar or more above their hydrostatic-pressure–volume curves. These results indicate that shear stresses with magnitudes of about 30–40 kbar persist in aluminum oxide to shock-pressure levels of at least 300 kbar.

INTRODUCTION

Knowledge of the dynamic yield behavior of polycrystalline aluminum oxide (alumina) is important because of the technical uses of this material. The Hugoniot elastic limit (HEL) and Hugoniot data immediately above the HEL for two polycrystalline forms of aluminum oxide are discussed here. The high-pressure behavior of alumina under hydrostatic stress has been reported by Bridgman[1] and by Hart and Drickamer[2] to 29 and 304 kbar, respectively. Hugoniot data for single and polycrystalline alumina at high stress levels (300–1500 kbar) have been reported by McQueen and Marsh.[3]

MATERIALS

Two alumina ceramics were investigated in this study. The series of experiments performed at the Stanford Research Institute (SRI) was on the G. E. high-density ceramic Lucalox,[4] and the series at the Lawrence Radiation Laboratory (LRL) was on a lower-density ceramic, which will be designated Wesgo Al-995.[5] Lucalox was studied since it has the highest density and purity (99.8%) of the commercially available alumina ceramics. Wesgo Al-995, on the other hand, appeared to be the highest density and purity alumina which could be easily cut or shaped by grinding or drilling. The purity of the Al-995 is greater than 99.5%, the major impurities being MgO and SiO_2. The porosity of the samples used ranged from 3.5%–4.3%, most samples being nearer the upper figure The porosity of the Lucalox was less than 0.2%.

The elastic moduli of Lucalox and the pressure and temperature derivatives of these moduli have been precisely measured to 4 kbar under hydrostatic pressure.[6] Elastic moduli for Wesgo Al-995 have also been measured.[7]

EXPERIMENTS

Plane shock waves are driven by a series of explosive systems (see Table I) through a driver plate of a standard material and then into a sample plate of aluminum oxide. Depending on the final shock stress level, one or two shock fronts form in the sample. When the level of the driving shock stress, σ_2, in the Lucalox is below ~600 kbar or in the Wesgo Al-995 below ~900 kbar, a precursor shock (or elastic shock) of amplitude σ_1 forms. The specimen is first shocked to stress amplitude σ_1 by the elastic shock and then to σ_2 by the following and more slowly propagating deformational shock. The stress amplitude of the elastic shock, called the Hugoniot elastic limit or HEL, represents the maximum normal stress that a material can withstand under one-dimensional compressive strain without internal rearrangement taking place at the shock front. Above 600 (or for the Al-995, 900) kbar the elastic shock is overdriven and only the deformational shock forms. The Hugoniot curve above the HEL thus represents the locus of states for which internal rearrangement, i.e., some type of yielding, has occurred in achieving the shock state. The shock stress and volume are computed from the measured shock and particle velocity and initial density, ρ_0, using the Rankine–Hugoniot conservation equations. The stress measured is, of course, the component in the shock propagation direction.

The primary experimental technique employed inclined mirrors, as shown in Fig. 1. For high shock pressures, where the elastic shock is overdriven, or

* Supported by U.S. Army Materials Research Agency and U.S. Atomic Energy Commission. Division of Geological Sciences Contribution No. 1502, California Institute of Technology.

† Present address: Seismological Laboratory, California Institute of Technology, Pasadena, Calif.

[1] P. W. Bridgman, Proc. Am. Acad. Arts. Sci **77**, 187 (1949).

[2] M. V. Hart and H. G. Drickamer, J. Chem. Phys. **43**, 2265 (1965).

[3] R. G. McQueen and H. M. Marsh, in *Handbook of Physical Constants*, S. P. Clark, Jr., Ed., (Geological Society of America, New York, 1966), Chap. 7.

[4] Lucalox, General Electric Co. Lamp Glass Div., Cleveland, Ohio.

[5] Wesgo Al-995, Western Gold and Platinum Corp., Belmont, Calif.

[6] E. Schreiber and O. L. Anderson, J. Am. Ceram. Soc. **49**, 184 (1966).

[7] H. L. Dunegan (private communication).

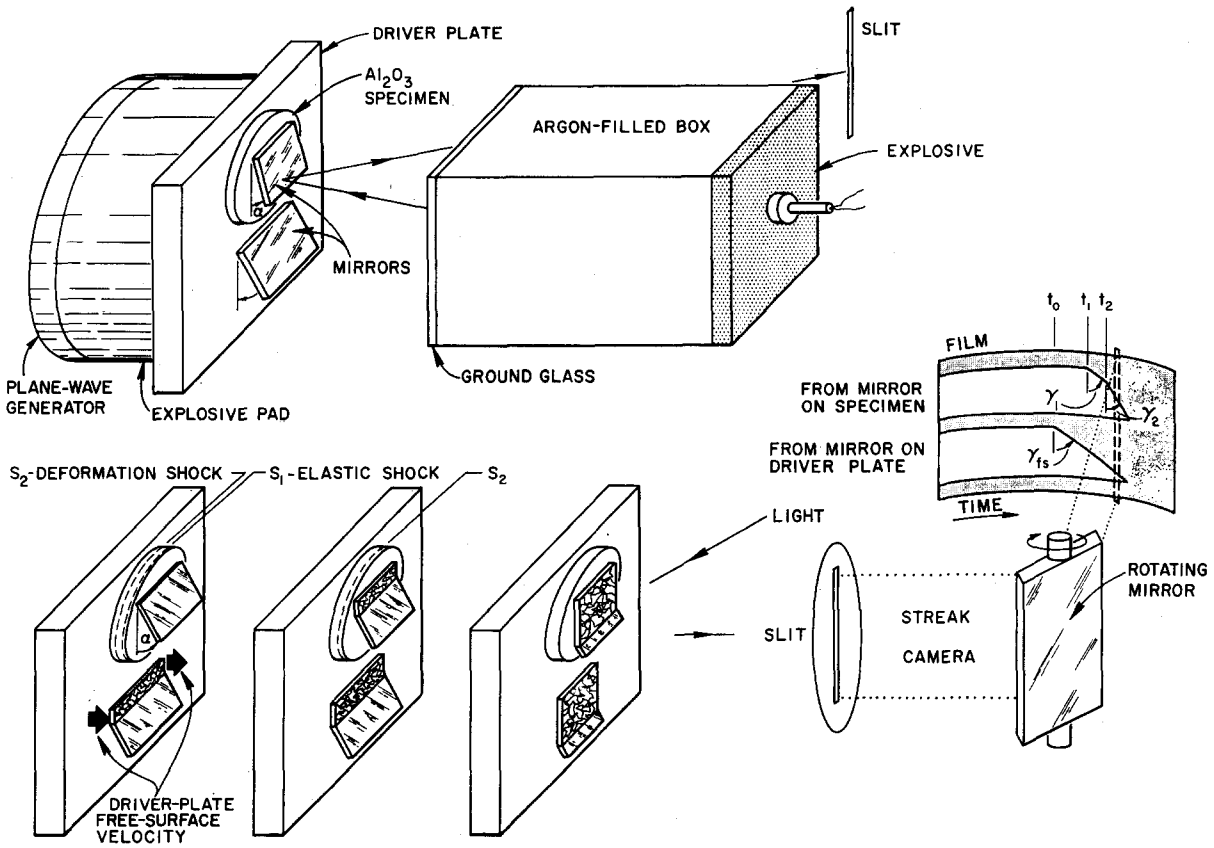

FIG. 1. Diagrammatic view of plane-wave–inclined-mirror experiment.

nearly overdriven, the free surface velocity of the driver plate and the shock velocity through the sample were measured. At these pressures, the impedance-matching technique[8] was used to obtain the shock state in the sample.

TABLE I. Explosive driver systems.

System	Components
A	*P* 80[a]+5.1 cm Baratol+1.9 cm 2024 aluminum
B	*P* 80+3.5 cm composition B-3+2.5 cm 2024 aluminum
C	*P* 120[b]+5.1 cm pressed TNT+1.3 cm brass+1.3 cm Lucite
D	*P* 120+15.2 cm pressed TNT+1.3 cm 2024 aluminum
E	*P* 120+10.2 cm PBX 9404+1.3 cm 2024 aluminum
F	*P* 120+15.2 cm pressed TNT+0.3 cm air+0.3 cm Monel+2.5 cm air+0.5 cm 256 brass
G	*P* 120+15.2 cm PBX 9404+0.3 cm air+0.3 cm Monel+2.5 cm air+0.4 cm 256 brass

[a] 20-cm-diam plane-wave lens.
[b] 30.5-cm-diam plane-wave lens.

[8] M. H. Rice, R. G. McQueen, and J. M. Walsh, in *Solid State Physics*, F. Seitz and D. Turnbull, Eds., (Academic Press Inc., New York, 1958), Vol. 6, pp. 1–63.

For shock pressures at which both an elastic and a deformational shock front form, the elastic and deformational shock velocities, U_1 and U_2, and the sample free-surface velocities, u_{1fs} and u_{2fs} were measured (Fig. 1). Figure 2 indicates that upon reflection of the elastic shock from the free surface of the sample, the free

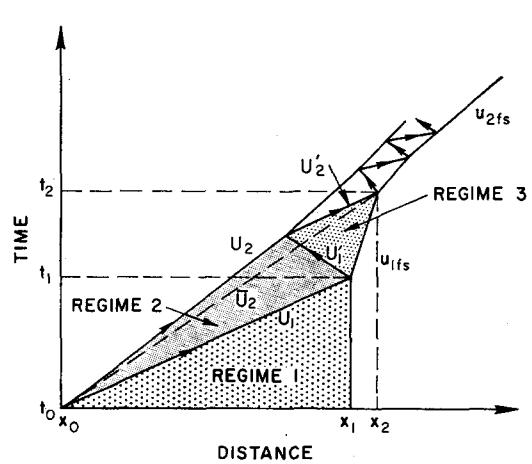

FIG. 2. Shock-wave paths in (x-t) plane. Material in regime 1 is unshocked in initial state; regime 2 represents elastic shock state; regime 3 represents material (moving at velocity u_{1fs}) which has been shocked into regime 2 and then returned to zero stress.

surface is accelerated to a velocity u_{1fs}. The inclined mirror on the sample loses its reflectivity as a result of interaction with the free surface, and a cutoff angle γ_1 results as the image of the mirror is swept along the film by the streak camera. Simultaneously the head of the resulting rarefaction wave propagates rearward at velocity U_1'. Upon interaction with the deformational shock, the stress of the oncoming shock is reduced and a wave with velocity U_2' arrives at the free surface at time t_2. A series of reflected rarefactions and oncoming shocks now rapidly accelerate the sample free surface to the velocity u_{2fs}, which is presumably characteristic of the deformational shock state in the sample. The various free-surface velocities of the sample, u_{1fs} and u_{2f} or of the driver plate, u_{fs}, are obtained from the formula

$$u_{fs}=W\tan\alpha/M\tan\gamma. \tag{1}$$

Here W and M are the streak camera writing rate and magnification, and α and γ are the initial inclined-mirror angles and inclined-mirror cutoff angles on the film, respectively. Corrections to these formulas are usually necessary to take into account deviations from ideal geometry.

In obtaining the particle velocity u_1 associated with the elastic shock state (regime 2), the free-surface approximation

$$u_1\cong u_{1fs}/2 \tag{2}$$

is assumed. The validity of Eq. (2) implies that the entropy increase associated with the shock state is small and that the material in regime 3 (Fig. 2) has the same properties as the material in regime 1. The shock stress and volume in the elastic shock state are then obtained by inserting u_1, U_1, and ρ_0 in the Rankine–Hugoniot conservation equations.

The deformational shock velocity U_2 is obtained from determining the time t_2 on the light cutoff pattern from the inclined mirror mounted on the sample. At this time the wave traveling at velocity U_2' is assumed to arrive at the free surface. The acceleration of the sample free surface, corresponding to an increase in velocity from u_{1fs} to u_{2fs}, presumably begins at this time. It follows from Fig. 2 that the deformational shock velocity U_2 is given by

$$U_2=\frac{U_1'(x_2-x_0)+U_2'(x_1-x_0)-U_1'U_2'(t_2-t_1)}{U_1'(t_1-t_0)+U_2'(t_2-t_0)-(x_2-x_1)}, \tag{3}$$

or

$$U_2=\frac{U_1'\bar{U}_2(U_1-u_{1fs})+U_2'U_1(\bar{U}_2-u_{1fs})-U_1'U_2'(U_1-\bar{U}_2)}{U_1'(\bar{U}_2-u_{1fs})+U_2'(U_1-u_{1fs})-u_{1fs}(U_1-\bar{U}_2)}, \tag{3a}$$

where the apparent shock velocity is given by

$$\begin{aligned}\bar{U}_2&=(x_2-x_0)/(t_2-t_0)\\&=[x_1-x_0+(t_2-t_1)u_{1fs}]/(t_2-t_0).\end{aligned} \tag{4}$$

Since for the present materials U_2 and U_1 have comparable values, the value obtained for U_2 is insensitive to the exact values of U_1', and U_2' used in Eq. (3). To be consistent with the approximation that the shock and rarefaction processes are nearly reversible [i.e., Eq. (2)], U_1' is usually taken to be equal to U_1-u_1. An appropriate value of U_2' must be assumed. One simple assumption is that

$$U_2'=U_1+u_{1fs}, \tag{5}$$

which implies that the interaction of the reflection of the first wave with the oncoming deformational shock is completely elastic. This should be strictly true if the final stress is less than twice the Hugoniot elastic limit, provided material is able to support the stresses associated with the elastic shock a second time. The insensitivity of U_2 in Eq. (3) to the values of U_1' and U_2' is evident from Table II. Only a small change in the deformational shock state results if the wave interaction is assumed to be such that $U_2'=U_2$. This is tantamount to assuming that in fact no wave interactions have occurred and that t_2 represents the time that the second shock would arrive at position x_2 if the free surface were not present.

When the two shocks form, the deformational-shock particle velocity is obtained using either the impedance-matching method (using an inclined mirror measurement of the driver free-surface velocity) or the sample free-surface velocity (and the free-surface approximation). Shock attenuation in the sample would tend to result in too high a particle velocity for a given shock velocity from the first method, and too low a particle velocity from the second method. The effect of these errors appears to be slight in that the data from the inclined mirror shots are consistent with each other and lie along the same curve as data obtained using the flash-gap method. Where the particle velocity can be obtained from both methods, they are comparable.

Measurements of both crystalline and ceramic alumina have been made by McQueen and Marsh[3] using the flash-gap technique. Further measurements[9] on the Wesgo Al-995 ceramic were made using the same technique at 218, 290, and 736 kbar and were in good agreement with the data of McQueen and Marsh. In these measurements, shock velocity was measured on

[9] Shots ESTER-292, 288, and 287, respectively. B. L. Hord (private communication).

TABLE II. Hugoniot data for aluminum oxide (Lucalox ceramic and Wesgo ceramic).

					First (elastic) shock state				Second (deformational) shock state					
Shot no.	Explosive system[a]	Initial density (g/cm³)	Specimen thickness (mm)	Driver free-surface velocity (mm/μsec)	Shock velocity U_1 (mm/μsec)	Particle velocity u_1 (mm/μsec)	Shock stress σ_1 (kbar)	Volume V_1 (cm³/g)	Apparent velocity $\overline{U}_2$ (mm/μsec)	Shock velocity U_2 (mm/μsec)	Free-surface velocity u_{2fs} (mm/μsec)	Shock stress[b] σ_2 (kbar)	Particle velocity[b] u_2 (mm/μsec)	Volume[b] V_2 (cm³/g)
12 136	A	3.98	3.167	1.543	10.98	(0.368)[c]	(161)	0.2428	9.08	8.80	1.174	200	0.477	0.2398
												199	0.475	0.2398
		3.98	6.375	1.543	10.98	0.262	114	0.2452	9.04	8.79	0.944	196	0.492	0.2388
												195	0.495	0.2385
		3.98	12.705	1.543	10.90	0.284	123	0.2447	8.83	8.53	0.957	196	0.493	0.2387
												195	0.495	0.2385
12 138	B	3.98	6.365	2.694	10.98	0.253	111	0.2455	9.72	9.60	(1.67)[c]	373	0.931	0.2279
												369	0.93	0.2277
		3.98	12.687	2.694	10.88	0.228	99	0.2460	9.50	9.36	(1.57)[c]	369	0.944	0.2270
												366	0.96	0.2262
PLMB-6	C	3.814	6.557	d	10.07	0.26	100	0.2554	7.31	6.75	0.58	108	0.29[e]	0.2544
												107		0.2542
		3.810	6.384	d	10.38	0.21	84	0.2572	8.16	7.83	0.62	115	0.31[e]	0.2540
												113		0.2538
PLMB-7	D	3.814	6.427	d	10.32	0.20	79	0.2572	7.72	7.26	1.74	275	0.87[e]	0.2343
												263		0.2328
		3.809	6.577	d	9.82	0.18	67	0.2578	7.82	7.54	1.70	265	0.85[e]	0.2352
												259		0.2343
PLMB-5	E	3.810	6.372	d	10.07	0.22	85	0.2567	8.75	8.62	2.56	436	1.28[e]	0.2248
												432		0.2243
		3.809	6.353	d	10.05	0.21	81	0.2570	8.72	8.59	2.52	428	1.26[e]	0.2253
												424		0.2248
ESTER-287	F	3.808	6.445	5.00	d	d	d	d	9.88	d	d	736	1.96	0.2106
PLMB-8R	G	3.837	6.389	4.840	f	f	f	f	11.03	11.03	5.193[e]	1121	2.677	0.1974
		3.839	6.504	4.779	f	f	f	f	10.90	10.90	5.285[e]	1131	2.687	0.1963

[a] See Table I.
[b] Two entries calculated, using $\overline{U}_2$ and $\overline{U}_2$, respectively.
[c] Less certain data.
[d] Not measured.
[e] Obtained assuming $u_2 = u_{2fs}/2$.
[f] First shock overdriven.

TABLE III. Relation of HEL to offset of Hugoniot.

Hugoniot elastic limit (HEL) σ_1 (kbar)	Poisson's ratio ν	Maximum shear stress τ_{max} (kbar)	Hugoniot offset $\Delta\sigma_h$ (kbar)
112(±13)	0.2363[a]	39	52
83(±5)	0.218[b]	30	40

[a] From Ref. 7.
[b] From longitudinal and transverse velocities of 10.34 and 6.21 mm/μsec.

6.4-mm-thick samples of the ceramic and driver plate material, the free-surface velocity was measured on 3.2-mm samples of the driver plate material. Thus, the free-surface velocity measurement was made at a point corresponding to the mean shock velocity. Possible errors from shock attenuation in the samples are, hence, minimized. The shock state in the driver is obtained from the measured shock and free-surface velocities for the driver material and the known equation of state for the driver. The shock state in the ceramic material is then obtained by the impedance-matching technique.

The states measured with the flash-gap technique above 400 kbar fall on the deformational (second) shock Hugoniot established by the inclined-mirror measurements. This shows that the 0.88-mm argon flash gaps did not produce light on the arrival of the initial wave. Approximate calculations of gap closure using the known free-surface velocities show that the sample free-surface motion does not act long enough to close the gap before arrival of the second wave. Hence, it is the final (deformational) states that are observed in these experiments. Below 400 kbar, both the present and McQueen and Marsh experiments yield too high a second-shock velocity, indicating that the first wave closed the gap before the arrival of the second wave. Accordingly, all flash-gap data below 400 kbar have been discarded.

RESULTS AND CONCLUSIONS

The Hugoniot data for G.E. Lucalox and Wesgo Al-995 alumina ceramic are shown in relation to other Hugoniot and hydrostatic pressure–volume data for aluminum oxide in Fig. 3. The precision of the shock and of the particle velocity measurements for the deformational shock front is generally better than ±1% and ±3%. The uncertainty of the first shock-state particle velocity is approximately ±4%. The present Lucalox and Al-995 Hugoniot data agree well with the earlier high-pressure deformational shock stress data of McQueen and Marsh[3] for aluminum oxide in single-crystal (sapphire) and ceramic form. The HEL as observed in four of the five specimens of Lucalox is 112±13 kbar. Similarly, the HEL of six specimens of Al-995 ceramic is 83±5 kbar. These values are not unexpectedly lower than the HEL of the single-crystal sapphire; this varies from 120–200 kbar, depending on crystallographic orientation.[10]

The elastic shock velocities, U_1, observed in the Lucalox experiments (10.88–10.98 mm/μsec) are within 1% of the longitundinal elastic wave velocities of 10.845 mm/μsec reported by Schreiber and Anderson.[6] For the Al-995 ceramic, the measured elastic shock velocities ranged from 9.82–10.38 mm/μsec. These agree reasonably well with the value of 10.34 mm/μsec for the longitudinal elastic velocity which was measured[7] on a representative sample. This agreement of the elastic shock velocities with the longitudinal elastic wave data serves as partial justification for the use of free-surface approximation to infer the elastic shock states.

For one-dimensional compression the stress determined in shock experiments is the stress normal to the shock front. This is denoted by σ_x. At the HEL its value is given by $\sigma_x=\sigma_1$. From elasticity theory, the stresses $\sigma_y=\sigma_z$, parallel to the wavefront, are related to σ_x by

$$\sigma_y=\sigma_z=[\nu/(1-\nu)]\sigma_x, \tag{6}$$

where ν is Poisson's ratio. The maximum shear stress is then

$$\tau_{max}=(\sigma_x-\sigma_y)/2 =[(1-2\nu)/(1-\nu)](\sigma_1/2). \tag{7}$$

The values of τ_{max} generated at the HEL shock state for Lucalox and ceramic are calculated (Table III) using

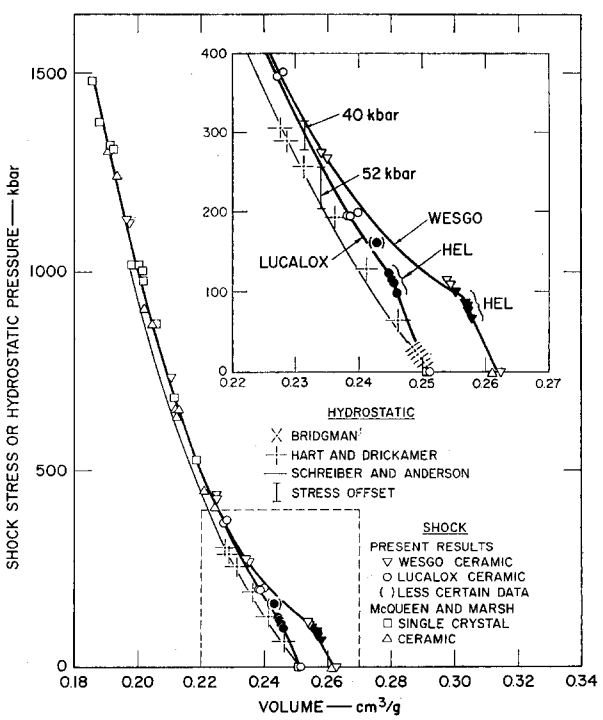

FIG. 3. Shock stress or hydrostatic pressure vs volume for various forms of aluminum oxide. Solid symbols indicate HEL states.

[10] W. P. Brook and R. A. Graham, Bull. Am. Phys. Soc. 11, 414 (1966).

the values of Poisson's ratio obtained from ultrasonic data.

The large offset in stress of the deformational Hugoniot curve for both ceramic and Lucalox above the room-temperature hydrostatic-pressure–volume curve suggests that both materials are able to support a substantial stress difference in the high-pressure shock state. In the Appendix, a calculation of shock heating on the Hugoniot is outlined. Calculations of the temperature rise and pressure offset of the Hugoniot from the isotherm resulting from shock heating are given in Table IV. These show that the offset of the deformational Hugoniot curve from the room-temperature hydrostatic-pressure–volume curve, the isotherm, can account for an offset of only a few kbar at several hundred kbar.

If the aluminum oxide ceramics retain their ability to withstand the *same* level of shear stress produced at the Hugoniot elastic limit when shocked to states along the deformational portion of the Hugoniot, their behavior may be characterized as that of a simple elastic–plastic solid.[8] In this case $\Delta\sigma_h=\sigma_x-p$ will be the offset of the deformational Hugoniot above the hydrostatic-pressure–volume curve. In general, the hydrostatic pressure is given by

$$p=\sigma_x-2(\sigma_x-\sigma_y)/3. \tag{8}$$

It follows from Eqs. (7) and (8) that the stress offset is given by

$$\begin{aligned}\Delta\sigma_h&=\sigma_x-p\\&=4\tau_{\max}/3\\&=[(1-2\nu)/(1-\nu)](2\sigma_1/3).\end{aligned} \tag{9}$$

The calculated stress offsets for Lucalox and Wesgo Al-995 ceramics are of similar magnitude. For Lucalox this result appears to fit the available data, at least below 300 kbar where a realistic comparison can be made with the Hart and Drickamer[2] results. For the porous Al-995 ceramic this result is comparable with the data only at ~300 kbar. Below this stress the Hugoniot is considerably offset above the hydrostatic curve for the single crystal. Additional experiments on two alumina ceramics having densities of 3.72 and 3.92 g/cm^3 have recently been carried out at the Lawrence Radiation Laboratory. Preliminary results indicate that these materials have HEL's of ~80 and ~140 kbar, respectively (comparable to those reported here). Their deformational Hugoniot curves also display a stress offset above the single-crystal hydrostatic-compression curve [W. H. Gust and E. B. Royce (in preparation)]. These offsets probably result from the material's initial porosity and the fact that several times the yield strength of a ceramic or porous rock is needed to completely collapse the void structure.[11] The adiabatic compression curve shown in Fig. 3 is calculated by fitting the Schreiber and Anderson ultrasonic velocity data[6] with a Murnaghan logarithmic equation.

[11] D. R. Stephens and E. M. Lilly, Lawrence Radiation Lab. Rept. UCRL-14711, (March 1966).

TABLE IV. Calculated temperature rise for shocked material on the Hugoniot and associated thermal-pressure offset of the Hugoniot from the 300°K isotherm.

Shock pressure (kbar)	G.E. Lucalox ΔT (C°)	G.E. Lucalox ΔP (kbar)	Wesgo Al-995 ΔT (C°)	Wesgo Al-995 ΔP (kbar)
250	60	2	210	10
500	190	8	420	24
1000	690	40	1140	72

The maximum shear stresses of 52 and 140 kbar obtained from the present experiments correspond to a strain rate of $\sim 2\times 10^5$ sec. This strain rate is obtained by dividing the value of the one-dimensional strain at the HEL, ~0.02, by the rise of the elastic shock, $\sim 10^{-7}$ sec. In previous experiments[12–14] performed on this and similar material at much lower strain rates (10^{-3}–10^{+3}/sec) and in differing geometries, the maximum shear stresses obtained were at least one order of magnitude lower than those of the present experiment. The experiments of Sedlacek,[14] show a small strain-rate effect at the highest strain rates employed.

However, these quasistatic tests are biaxial stress tests, in which one of the three principal stresses is, or is close to, zero. The one-dimensional strain compression characterizing shock loading is essentially a triaxial loading, in which all three principal stresses are large.

An extension of the brittle fracture model applicable for homogeneous media, such as a glass, to an inhomogeneous medium, such as a ceramic, has been constructed by Holt.[15] In his model $\tau_{\max}$ is a function of p, the mean principal stress. Such a model can successfully fit the biaxial yield data[13] for various stress configurations (tension, compression, and mixed modes) as well as predict a value for the Hugoniot elastic limit. For Wesgo Al-995, a Hugoniot elastic limit approximately 20% lower than the experimental value is predicted. Thus, the high resolved shear stress characterizing yield under shock conditions is a result primarily of the triaxial character of the loading, as contrasted to the biaxial loading characterizing the usual static yield experiments. A small strain-rate effect, as seen in the experiments of Sedlacek[14] may explain the failure of Holt's brittle fracture model to predict the exact value of the Hugoniot elastic limit.

[12] N. M. Parikh, Tech. Rept. to Air Force Materials Lab., ASD-TR-61-628-III, (June 1964).

[13] L. J. Broutman and R. H. Cornish, J. Am. Ceram. Soc. **48**, 519 (1965).

[14] R. Sedlacek, Tech. Rept. to Air Force Materials Lab., AFML-TR-65-129, (August, 1965).

[15] A. C. Holt, Bull. Am. Phys. Soc. **12**, 1130 (1967), and private communication.

ACKNOWLEDGMENTS

The work carried out at Lawrence Radiation Laboratory was performed under the auspices of the U.S. Atomic Energy Commission. The work at Stanford Research Institute was in part supported by the Army Materials Research Agency. The inclined-mirror experiments were carried out with the assistance of M. J. D'Addario, C. A. Falco, J. W. Schimmel, and W. C. Mumper at LRL. The flash-gap experiments were performed by B. L. Hord. The program at SRI was initiated by A. F. Florence and experiments were carried out by J. T. Rosenberg. Calculations of the temperature and of the isotropic compression curve from ultrasonic data were independently performed by Richard Grover. Our understanding of the failure mode in ceramics has been greatly improved by conversations with Albert C. Holt.

APPENDIX: HUGONIOT TEMPERATURE CALCULATIONS

The procedure used in calculating temperatures on the Hugoniot is similar to that outlined in Refs. 8 and 16 and is primarily the work of R. Grover and F. J. Rogers of LRL.

Write the equation of state relating pressure P, volume V, and energy E in the Grüneisen form,

$$P(V,E)=P_K(V)+\gamma(V)[E-E_K(V)]/V. \quad \text{(A1)}$$

The energy on the 0°K isotherm (or isentrope) is related to the pressure on the 0°K isotherm (or isentrope) by

$$E_K=-\int_{V_0}^{V} P_K dV. \quad \text{(A2)}$$

The specification of $P_K(V)$ and $\gamma(V)$ then provides a complete $P(V, E)$ equation of state. The calculation of a temperature requires an additional assumption concerning the specific heat at constant volume, $C_V(V, T)$.

In the present calculations, the pressure and energy in Eq. (A1) are replaced by their experimental values on the Hugoniot $P_H(V)$ and $E_H(V)$, and $E_K(V)$ is written in terms of $P(V_K)$ as in Eq. (A2), yielding a relation between $P_K(V)$ and $\gamma(V)$. Gruneisen's gamma $\gamma(v)$ is then assumed in the Dugdale–MacDonald form

$$\gamma(V)=-\tfrac{1}{3}-(V/2)(d^2/dv^2)[P_K(V)V^{2/3}]/(d/dV)[P_K(V)V^{2/3}], \quad \text{(A3)}$$

the result being a differential equation for $P_K(V)$. This equation is integrated numerically to yield $P_K(V)$, $E_K(V)$, and $\gamma(V)$. (The actual integration is done for $E_K(V)$ rather than $P_K(V)$, for convenience.) The use of Slater's formula for $\gamma(V)$ or the assumption that $\gamma(V)/V$ is constant give results similar to those for the Dugdale–MacDonald gamma. This is true because $\gamma(V)$ need not be known very accurately at low pressures, the Hugoniot and isentrope being almost identical. At high pressures, the various formulas all give comparable values of gamma.

The temperature on the Hugoniot is obtained by an appropriate integration[17] of the thermodynamic identity

$$TdS=C_V dT+T(\partial P/\partial T)_V dV. \quad \text{(A4)}$$

The specific heat C_V is taken to be a function of volume and temperature in the following way. The temperature dependence of C_V is assumed in the Debye form, and the Debye temperature θ_D is made volume-dependent by the relation

$$\gamma(V)=-\partial \ln\theta_D(V)/\partial \ln V. \quad \text{(A5)}$$

The calculation, as outlined so far, follows the ideas in Refs. 8 and 16. The application of such a procedure to alumina involves adding corrections for two effects; (1) the strength of the material and consequent offset of the Hugoniot from the isotropic compression curve, and (2) the porosity of the Wesgo ceramic. The offset of the experimental Hugoniot from the isentropic compression curve was taken into account by performing the calculations for a fictitious "isotropic Hugoniot." This curve is parallel to the experimental Hugoniot above the elastic limit but offset from it in the (P, V) plane so that it passes through the correct initial density. Unlike the experimental Hugoniot, it is characterized by a linear (U_s, U_p) relation.

Since the porosity of the Wesgo ceramic is small, the Hugoniots for the porous and nonporous materials should be expected to be essentially identical at high pressures in the (P, V) plane. For the purpose of calculating the correction to the temperature due to the porosity, the two Hugoniots are assumed to coincide in the P–V plane. The additional temperature of the shocked porous material over the shocked nonporous material is then $\delta T=P(\delta V)/2C_V$, where δV is the difference in initial specific volume of the porous and nonporous material. Similarly, the additional pressure is $\delta P=\gamma P(\delta V)/2V$. Though the correction to the Hugoniot pressure is small (justifying the initial assumption), the correction to the shock-induced temperature rise is comparable to the temperature rise of the nonporous material.

[16] R. G. McQueen and S. P. Marsh, J. Appl. Phys. 31, 1253 (1960).

[17] J. M. Walsh and R. H. Christian, Phys. Rev. 97, 1544 (1955).